



**HAL**  
open science

## Solid-state emitters presenting a modular excited-state proton transfer (ESIPT) process: recent advances in dual-state emission and lasing applications

Martyna Durko-Maciag, Gilles Ulrich, Denis Jacquemin, Jaroslaw Mysliwec,  
Julien Massue

### ► To cite this version:

Martyna Durko-Maciag, Gilles Ulrich, Denis Jacquemin, Jaroslaw Mysliwec, Julien Massue. Solid-state emitters presenting a modular excited-state proton transfer (ESIPT) process: recent advances in dual-state emission and lasing applications. *Physical Chemistry Chemical Physics*, 2023, 25 (22), pp.15085-15098. 10.1039/D3CP00938F . hal-04283038

**HAL Id: hal-04283038**

**<https://cnrs.hal.science/hal-04283038v1>**

Submitted on 13 Nov 2023

**HAL** is a multi-disciplinary open access archive for the deposit and dissemination of scientific research documents, whether they are published or not. The documents may come from teaching and research institutions in France or abroad, or from public or private research centers.

L'archive ouverte pluridisciplinaire **HAL**, est destinée au dépôt et à la diffusion de documents scientifiques de niveau recherche, publiés ou non, émanant des établissements d'enseignement et de recherche français ou étrangers, des laboratoires publics ou privés.

# **Solid-State Emitters Presenting a Modular Excited-State Proton Transfer (ESIPT) Process: Recent Advances in Dual-State Emission and Lasing Applications**

Martyna Durko-Maciąg,<sup>[a]</sup> Gilles Ulrich,<sup>[b]</sup> Denis Jacquemin,<sup>[c]</sup> <sup>[d]</sup> Jaroslaw Mysliwiec<sup>[a]\*</sup> and Julien Massue<sup>[b]\*</sup>

<sup>[a]</sup> Wroclaw University of Science and Technology, Wyspianskiego 27, 50-370 Wroclaw, Poland

<sup>[b]</sup> Institut de Chimie et Procédés pour l’Energie, l’Environnement et la Santé (ICPEES), Equipe Chimie Organique pour la Biologie, les Matériaux et l’Optique (COMBO), UMR CNRS 7515, Ecole Européenne de Chimie, Polymères et Matériaux (ECPM), 25 Rue Becquerel, 67087 Strasbourg Cedex 02, France

<sup>[c]</sup> Nantes Université, CNRS, CEISAM UMR 6230, F-44000 Nantes, France

<sup>[d]</sup> Institut Universitaire de France (IUF), F-75005, Paris, France

Emails: [jaroslaw.mysliwiec@pwr.edu.pl](mailto:jaroslaw.mysliwiec@pwr.edu.pl), [massue@unistra.fr](mailto:massue@unistra.fr)

## Abstract

This review aims at providing a broad readership of material and physical chemists, as well as those interested in ab initio calculations, about recent advances in the fields of dual solution-solid emitters and lasing applications based on organic dyes displaying an excited-state intramolecular proton transfer (ESIPT) process. ESIPT is known to be highly sensitive to the immediate environment leading to the engineering of a wide range stimuli-responsive fluorescent dyes. With the structural diversity of ESIPT-capable fluorophores being large, many applications have been targeted over the years in the fields of optoelectronics, biology and luminescent displays. This review wishes to point out two emerging applications concerning ESIPT fluorophores, which are the quest for emitters fluorescing both in solution and solid, and those capable of light amplification.



## Introduction

Proton transfer is ubiquitous in nature and is at the origin of numerous biological regulation processes within living organisms but it has also been employed in molecular material science to engineer responsive organic molecules where a signal or information can be conveyed along a  $\pi$ -conjugated molecular scaffold.<sup>1</sup> Among the various possibilities of prototropy, Excited-State Intramolecular Proton Transfer (ESIPT) consists in an ultrafast phototautomerization, in the subpicosecond scale between a photoexcited normal ( $N^*$ ) isomer and its corresponding tautomeric species ( $T^*$ ). ESIPT is commonly observed in heterocyclic  $\pi$ -conjugated molecules of natural or synthetic origin, containing a strong internal hydrogen bond embedded within five- or six-membered rings<sup>2</sup> While a range of proton donors and acceptors of different nature can be found in the literature, a large number of cases narrow down the ESIPT process to an enol ( $E^*$ )/keto ( $K^*$ ) tautomerism occurring upon photoexcitation. ESIPT induces a strong reorganization of the molecular geometry of the dyes in the excited-state leading to a fluorescence response presenting large Stokes shifts (up to  $12,000\text{ cm}^{-1}$ ), thereby limiting reabsorption processes and subsequent inner filter effect, that both often yield to detrimental photobleaching.<sup>3</sup> Additionally, while the vast majority of organic fluorescent dyes are only emissive in dilute solution and not in the solid-state due to aggregation-caused quenching (ACQ) processes,<sup>4</sup> ESIPT fluorophores are usually faintly luminescent in solution but strongly brighten up when molecular motions are restricted. In a similar fashion, Aggregation-Induced Emission (AIE) corresponds to the fluorescence enhancement upon restriction of molecular rotations;<sup>5</sup> and this increasingly popular feature can be further augmented by the introduction of ESIPT centers on the core of the AIE dyes.<sup>6</sup> ESIPT emitters have long been known as attractive solid-state emitters, with adaptive optical profiles depending on environment, *e.g.* amorphous powders, crystals, polymeric thin films or embedded in various matrixes, such as nanoparticles or aggregates.<sup>7</sup> Indeed, another characteristic of ESIPT fluorescence lies in its strong sensitivity to the immediate environment.<sup>8</sup> Intramolecular prototropy can indeed compete with other processes depending on the physical nature of the environment, strongly impacting the optical properties. As a result, synthetic organic fluorophores displaying an ESIPT process have been studied with the view to benefit from the competitive dynamics occurring between the various possible excited-states, which paves the way to the engineering of environment-responsive molecular switches (Figure 1).<sup>9</sup> Indeed, as the ESIPT process is typically under thermodynamic control, one possibility is that the ultrafast population of the  $K^*$  could lead to an equilibrium with a stabilized low-lying  $E^*$  state, leading to a dual  $E^*/K^*$  emission.<sup>10</sup> Dual emitters with adaptable intensity ratios between emission bands are good candidates for ratiometric detection,<sup>11</sup> panchromatic monomolecular white fluorescence,<sup>12</sup> and can be applied in optoelectronics devices, as well as security cryptographic inks. Additionally, organic dyes with intramolecular hydrogen bond and a structure showing a strong push-pull character can also trigger a competition between ESIPT and Excited-State Intramolecular Charge Transfer (ESICT) processes, which can even lead to the full frustration of the proton transfer.<sup>13</sup> Finally, in dissociative media, a full or partial competition with deprotonation can also be observed, producing anionic species,

some showing particularly intense fluorescence.<sup>14</sup> All these processes can simultaneously compete to produce fluorophores with complex emission profiles highly dependent on the polarization of their close environment (Figure 1).<sup>15</sup> Literature is rich of examples of H-bonded ESIPT-capable dyes with 5-, 6-membered rings or more in their molecular backbone,<sup>16</sup> yet the 2-(2'-hydroxyphenyl)benzazole (HBX, with X = NR, benzimidazole (HBI), X = O, benzoxazole (HBO) and X = S, benzothiazole (HBT)) fluorophores remain the most studied families of dyes displaying ESIPT, owing to their ease of synthesis and synthetic modification, versatility and possibility to induce drastic optical changes upon small molecular inputs.<sup>17</sup>

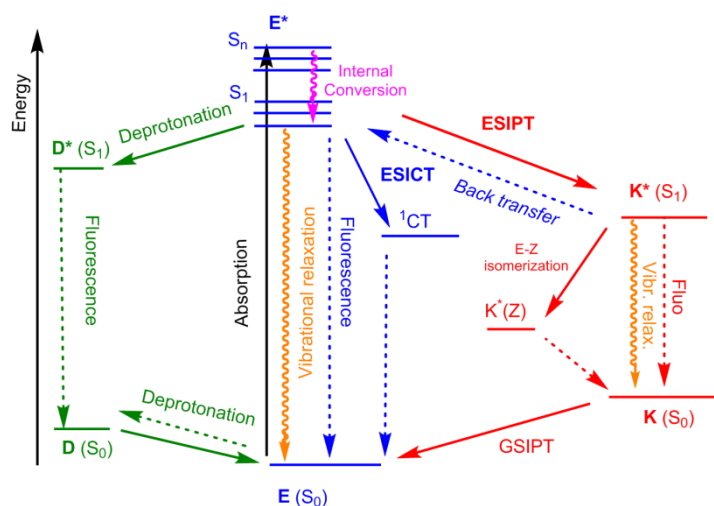


**Figure 1.** Schematic representation of the ESIPT process, along with selected other competitive processes.

Recently, there has been a global interest in the engineering of fluorophores, capable of displaying strong emission both in dilute solution and in the solid-state. This class of compounds, called dual-state emission (DSE) fluorophores or Solution and Solid-State Emitters (SSSE) have emerged as promising alternatives to fill the gap between the systems relying on either ACQ or AIE processes, as they allow targeting a wider range of applications in the fields of biotechnologies or optoelectronics. Several recent excellent reviews already compiled examples and mechanisms underlying the photophysics of these compounds.<sup>18</sup> For all the reasons aforementioned, ESIPT process can play a preeminent role in optimizing DSE properties of existent dyes but also in the search of original compounds; the current challenge being the increase of fluorescence intensity in solution while keeping strong emission quantum yield in solid. In this context, theoretical calculations appear as a tool of choice for rationalizing and understanding the properties of such compounds. In parallel, lasing has also proved to be an important field of application for organic dyes. Indeed, lasers stand out due to their remarkable properties, which allowed for the accelerated development of many fields, ranging from various areas of applied science, through commercially available household appliances, to medical applications.<sup>19</sup> In response to such a large demand for lasers, it appeared necessary to optimize and improve the properties of the devices themselves, by searching for new active organic materials capable of amplifying light and understanding the processes taking place and notably, the conditions for obtaining a population inversion. In this context, ESIPT process, due to its four-level system offers as an attractive possibility to

upgrade or optimize the properties of laser dyes, while offering a stronger degree of modularity. As a result, research on ESIPT-capable lasing dyes is currently very active.

This mini review aims at updating the reader on recent advances in these two emerging fields of research (DSE dyes and organic lasing based on ESIPT fluorescence) which have seen recent remarkable developments where ESIPT-capable fluorophores lead to an improvement of technologies and can further help tackle important future challenges.

## Dual-State Emission

### *General considerations and recent examples*

As mentioned in the Introduction, DSE processes correspond to dyes showing emission both in solution and in the solid state, which can therefore target a wider range of applications than the majority of structures based on either ACQ or AIE processes that are typically non or very poorly emissive in one of the two environments. There are no identified ground rules for the elaboration of DSE materials, although a few trends have already emerged. Indeed, many DSE fluorophores arise from a combination within the same backbone of a planar aromatic core, prone to ACQ, judiciously substituted with AIE units aiming at increasing solid-state fluorescence. DSE process is therefore obtained from a tenuous compromise between quasi-planarity, semi-rigidity, and solubility. The presence of heteroatoms on the  $\pi$ -conjugated scaffold of DSE dyes is also frequently observed, inducing intramolecular charge transfer (ICT) within the structures, creating dipole moments, therefore promoting significant geometrical reorganization between the ground and excited states.

The majority of DSE fluorophores are non-ESIPT heterocyclic scaffolds, and examples can be found in several hallmark dye families, e.g., triphenylamine,<sup>20</sup> phthalamides,<sup>21</sup> benzo[1,2,5]thiadiazole,<sup>22</sup> boron complexes,<sup>23</sup> or arenes.<sup>24</sup> As mentioned earlier, the main challenge appears to be the reduction of fluorescence quenching in solution, while maintaining solid-state emission. The key parameters to efficiently combine ESIPT and DSE seem to arise from an increase of rigidity by the reducing molecular motions, combined to a drastic reduction of the accessibility of the conical intersection (CI) related to the twisted intramolecular charge transfer (TICT) process often taking place after ESIPT. Obviously, the presence of a low-lying CI typically quenches the fluorescence. Restricting the access to CI(s) has been proposed as a key strategy for the engineering of DSE fluorophores, by strongly diminishing the related non-radiative excited-state deactivations in solution.<sup>25</sup> Among reported ESIPT-capable fluorophores, HBX dyes with DSE properties have also been reported in recent literature (Figure 2a). Recent examples of simple derivatization of the HBX scaffold have been particularly efficient for improving solution-state fluorescence while maintaining strong quantum yield values in solid. Notably, a series of ethynyl-extended HBX dyes indicated a significant effect of both rigidification and delocalization at selected position of the phenol ring (Figure 2b).<sup>26</sup> Another straightforward alternative to engineer HBX with DSE properties is to introduce one or two pyridine rings. It was found to be

an expedite way to reduce CI processes and restore fluorescence in solution; a feature which can be further enhanced by formation of the corresponding pyridinium moieties (Figure 2c).<sup>27</sup> The authors state that introduction of pyridine rings favors the stabilization of a merocyanine-like species in the excited-state, strongly decreasing non-radiative deactivations. According to *ab initio* calculations, N-methylpyridinium were able to stabilize the K\* state and subsequently disfavor non-radiative deactivations. Unfortunately, introduction of a cationic species led to enhanced fluorescence quenching of emission in the solid, owing to unfavorable cation- $\pi$  interactions, opening non-radiative deactivation channels. Very recently, it was shown that double introduction of both ethynyl extension and pyridine or pyridinium triggered a cooperative effect for the engineering of DSE properties (Figure 2c).<sup>28</sup> Five-membered oxazoline rings are structurally analogous to benzoxazole rings, yet with a stronger degree of flexibility, have been reported to display DSE emission. Göbel *et al* studied the influence of electronic substitution on this minimalistic ESIPt fluorophore, notably considering strong electrowithdrawing substituents (CF<sub>3</sub>, CO<sub>2</sub>Me).<sup>29</sup> The same team also reported nitrile-substituted 2-(oxazoliny)-phenols where the position of the nitrile substituents induced different effects (Figure 2d).<sup>30</sup>

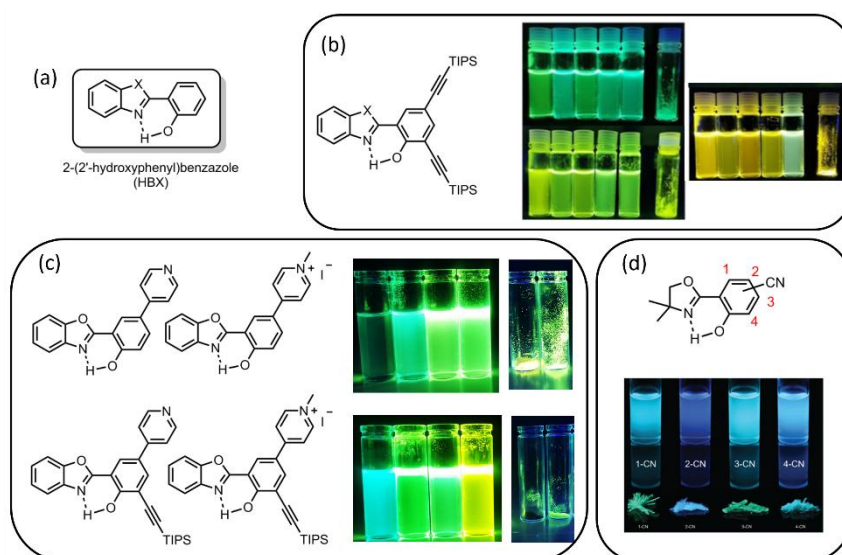


**Figure 2.** Examples of derivatization of the HBX core with (a) Unsubstituted HBX dyes. (b) Ethynyl-extended trialkylsilane HBX dyes (photographs corresponds to HBI, HBO and HBT dyes in solution in different solvents). (c) Pyridine or pyridinium-substituted HBX dyes (solutions at the top correspond to pyridine-substituted dyes and solutions at the bottom correspond to pyridinium-substituted dyes) (d) Introduction of cyano moieties on the scaffold of phenol-oxazoline rings.<sup>26-30</sup> Adapted from Ref. 26b Copyright 2021 John Wiley and Sons. Adapted from Ref. 28 Copyright 2022 Elsevier. Adapted from Ref. 30 Copyright 2020 the Royal Society of Chemistry.

Other examples of ESIPt/DSE dyes within the HBX family include rigidified benzimidazole derivatives, including N-arylated 9,10-phenanthroimidazole<sup>31</sup> or an example by Takagi *et al* where fluorescence intensity

can be enhanced by introduction of supramolecular H-bonded rigidification.<sup>32</sup> The same group also investigated the influence of structural rigidification by ring fusion on the optical properties of the resulting dyes.<sup>33</sup> Among the HBX family, benzothiazole-based derivatives (HBT) have been particularly scrutinized, due to the electrodonating nature of sulfur, leading to redshifted emission, making them better candidates for biological applications. Notably, a dual-channel fluorescent HBT probe for the logic-based visualization of aging biomarkers (thiophenol and hypochlorous acid HCOCl) was developed.<sup>34</sup> Moreover, Kaur *et al* a delocalized HBT dye with a styryl spacer capable of tuning the emission color over a wide range.<sup>35</sup> Other organic scaffolds showing both ESIPT and DSE properties can be found in the recent literature (Figure 3). Notable examples include imidazolo[5,4-*b*]thieno[3,2-*e*]pyridine derivatives, where the DSE properties are explained by a finely controlled self-assembly and a restriction of TICT processes.<sup>36</sup> A double H-bonded 2,2'-bipyridine-3,3'-diol-5,5'-dicarboxylic acid ethyl ester has been reported as a single ESIPT emitter while the other hydrogen bond participates in the rigidification of the overall scaffold, making this dye suitable for an insertion in OLED devices.<sup>37</sup> Other examples include 2,5-disubstituted-1,3,4-oxadiazoles<sup>38</sup> and most importantly red/NIR emissive squaraine derivatives.<sup>39</sup> Guided by TD-DFT calculations, the authors demonstrate that the removal a simple phenyl ring led to intense red/NIR emissions in solution and in crystals. A subtle alleviation of the TICT mechanism within the structure of these dyes appears to be at the origin of these attractive photophysical properties.

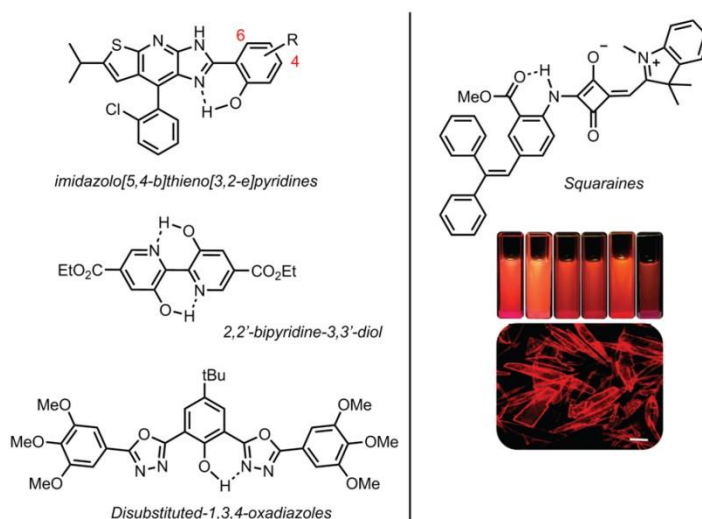


**Figure 3.** Examples of miscellaneous ESIPT fluorophores showing DSE properties.<sup>36-39</sup> Adapted from Ref. 39  
Copyright 2020 the Royal Society of Chemistry.

### First-principle calculations

As for all excited-state processes relying on ultra-fast processes, theoretical modelling is often used to shed a complementary light onto the experimental results. Indeed, theory can rather straightforwardly provide some key information, such as the excited-state geometries, that can typically not be determined with experimental approaches. For the specific case of ESIPT dyes, as illustrated by the above discussion, two specific aspects are challenging for theory: *i*) the relative energies of the tautomers should be determined with high accuracy;



ii) a proper modelling of the environment is often required to reach valuable insights, since both the proton-transfer itself, and the emission properties of the two tautomers are significantly tuned by the medium. The purpose of this section is to describe selected examples of works that have been focused on capturing these environmental effects, which is of high relevance for DSE, so that we do not describe gas phase calculations below. For a more general discussion regarding both the theoretical methods and computational strategies that can be used to describe ESIPT dyes, we refer the interested readers to the excellent 2021 review of Jankowska and Sobolewski, who provided an overview of these approaches as well as interesting advices for properly modelling ESIPT in organic dyes.<sup>40</sup> In the two next paragraphs, we describe methods available for the solvated and solid-state case.

For modelling ESIPT emission in solution, most works rely on so-called continuum solvation models, the most well-known being the Polarizable Continuum Model (PCM) originally developed in Pisa and implemented in several popular quantum chemistry packages.<sup>41</sup> In continuum approaches, the environment is represented as a structureless medium having the key physical features of the actual macroscopic solvent, and such computational strategy is very computationally effective, although it cannot accurately describe specific solute-solvent interactions, and is therefore not well-suited for protic solvents that tend to form hydrogen bonds with the ESIPT dye. For non-protic medium, PCM and other similar models, offer a generally excellent compromise between computational effort and quality of the results. Various continuum models have been coupled with a wide variety of excited-state electronic structure approaches,<sup>42</sup> and one specific aspect needs to be addressed: the nature of the coupling between the solution and the excited-state. One can roughly split the solvent models into the *linear-response* and *state-specific* approaches.<sup>43</sup> The former *linear-response* contribution stems from the coupling between the transition dipole moment and the solvent, and the magnitude of this contribution is therefore roughly dependent on the transition probability (oscillator strength).<sup>44</sup> In other words, *linear-response* effects are large for bright transitions. The latter contributions depends upon the change of polarity of the compound during the investigated electronic transition, and its magnitude is therefore roughly linked to the change of dipole moment between the two states, *i.e.*, *state-specific* effects are significant for transitions involving significant charge-transfer.<sup>45</sup> For ESIPT dyes, the enol and keto forms have often vastly different emission signatures, the former being both more polar and more dipole-allowed than the latter, at least in most HBX derivatives. This specific feature of ESIPT dyes motivated one of us to propose a computational protocol that includes simultaneously these *linear-response* and *state-specific* effects, an approach that is denoted cLR<sup>2</sup>-PCM (cLR stands for corrected linear response).<sup>46</sup> A typical example of the application of this model can be found in Figure 4 where we report keto-enol fluorescence differences for two dyes solvated in toluene, a solvent that would likely be considered as yielding rather mild changes as compared to gas. One nevertheless notes that the gas phase K<sup>\*</sup>-E<sup>\*</sup> shifts are too large as compared to experiment. Interestingly, both the *linear-response* (LR) and *state-specific* (cLR) models do provide corrections in the expected direction, which is the logical consequence of larger corrections for the enol structure than for the keto one. This is related to the fact that the fluorescence transition in E<sup>\*</sup> is both more

dipole-allowed (oscillator strength 20 times larger for the compound displayed on the left-hand side of Figure 4) and originating from a much more polarized state (twice larger excited-state dipole for the same compounds) than its  $K^*$  counterpart, inducing both large (small) *linear-response* and *state-specific* corrections for  $E^*$  ( $K^*$ ). As can be seen for one of the two compounds, only the use of  $cLR^2$  therefore allows reproducing the experiment in a satisfying manner, whereas both LR and  $cLR^2$  are successful for the other, in which the charge-transfer is more limited. Of course, more refined solvation models, allowing to capture specific solute-solvent interactions have been successfully applied to ESIPT as well.<sup>47</sup> As noted above, the emission efficiency of ESIPT HBX dyes is closely related to the accessibility of a low-lying CI corresponding to the interring twisting after ESIPT took place, similar to a TICT process. This CI was originally evidenced by theoretical calculations performed in the gas phase,<sup>48</sup> but is now well-recognized to be the key one in both solution and in the solid-state.

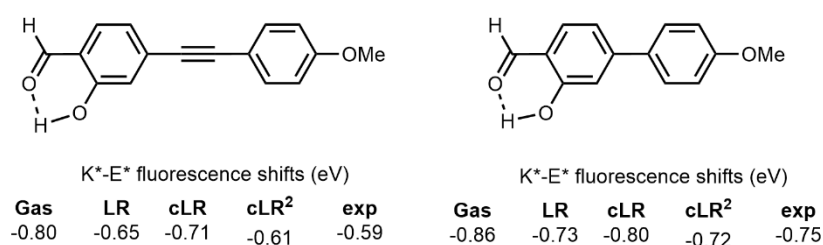


**Figure 4.** Illustration of the various solvent effects for two ESIPT dyes solvated in toluene. The reported values are the difference between the  $K^*$  and  $E^*$  emission energies for the two displayed dyes. See Ref. 46b for more details regarding the levels of theory used.

Whilst the actual description of the CI in itself requires using a multi-reference method that is typically too computationally demanding for large compounds, it has been suggested by some of us that one can explore the barrier separating the  $K^*$  from the CI with simpler approaches. To illustrate this point, we selected the calculations performed in Ref. 14a for substituted HBO dyes, and summarized in Figure 5. Considering the values determined in toluene, one notices a clear correlation between the computed twisting barriers and the measured quantum yields, the largest (smallest) calculated barrier being associated with the brightest (darkest) compound. Although this work relied on a continuum model, one notices that the qualitative correlation pertains in ethanol. This illustrates that rather straightforward calculations can be used to qualitatively explain, and hopefully predict, some experimental trends. We nevertheless wish to close this paragraph by a word of caution: such standard TD-DFT calculations are certainly not sufficient to provide quantitative estimates of emission yields, and one should always keep a critical eye on simplified theoretical modelling of complex phenomena.

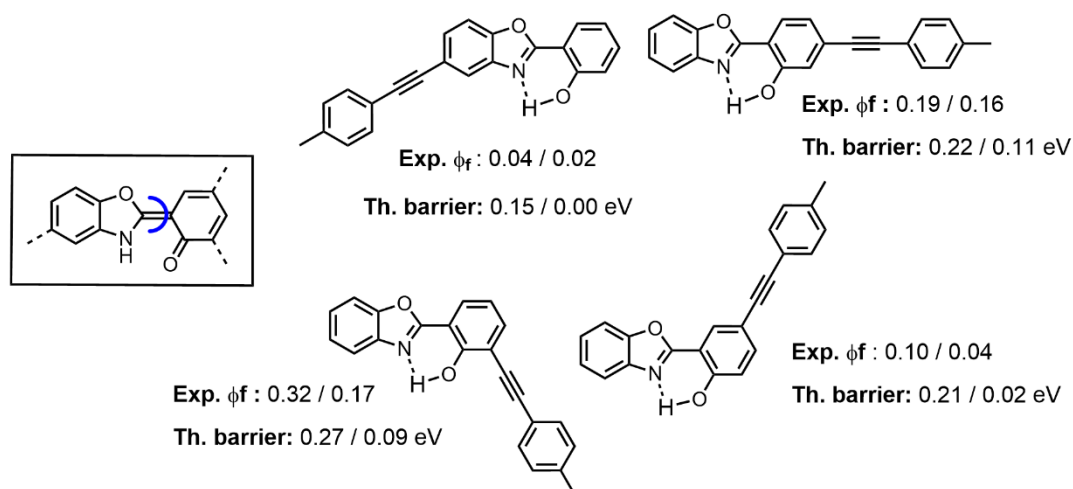


**Figure 5.** Comparison between the emission quantum yields measured in solution and the computed inter-ring twisting barrier for the  $K^*$  from for four ES IPT dyes showing DSE. We report data in both toluene and ethanol (Tol/EtOH). Data extracted from Ref. 14a.

For investigating ES IPT dyes in the solid-state, one should resort to different theoretical protocols as continuum models are generally not adequate; there are also different schemes when considering the dye in a crystalline environment or embedded in an amorphous (polymer or other) matrix. Modelling optical properties of organic compounds in these environments is difficult, especially for emission, yet very elegant protocols have been set up for the solid state, notably by the Adamo-Ciofini<sup>49</sup> and Crespo-Otero teams.<sup>50</sup> Their approaches have in common to split the problem into the dye and its environment, the latter being treated through a simplified quantum mechanics scheme, *i.e.*, a QM/QM' model, in which the polarization of the QM' environment part is self-consistently determined as a function of the excited-state density of the QM part (the dye), allowing a proper modeling of one of the key aspects influencing fluorescence. These approaches, or simpler ones relying on QM/MM rather than QM/QM', have been applied to model a variety of ES IPT dyes in the solid-state.<sup>49a-b, 50c, 51</sup> These studies provided insights not only into the origins of the shifts of the emission band upon changing environment, but also on the precise AIE mechanism. For instance, the authors investigated the ES IPT-able dye 2'-hydroxychalcone in its crystal state.<sup>51a</sup> This study showed that strong electrostatic interactions are detrimental for fluorescence, that is also influenced by the distortion of the crystal. It also provided insights into chemical strategies for maximizing the solid-state emission of ES IPT dyes: *i*) one can stabilize  $E^*$  (as compared to  $K^*$ ) as the non-radiative pathways are less effective in the enol form, yet this would require creating  $E^*$  with a large Stokes shift; *ii*) alternatively one can hinder the access to the CI in  $K^*$  by introducing fused rings preventing torsion/pyramidalization of the dye after ES IPT. In a more recent investigation performed with a large panel of high-level quantum chemical models, the same group treated a dozen of crystals built with ES IPT dyes and could explain all major experimental outcomes regarding the efficiency of the solid-state emission, as well as provide a series of rather generic design rules.<sup>50c</sup> Figure 6, reproduced from that work, illustrates how the accessibility to the key CI discussed above strongly differs in gas phase and in the crystal.

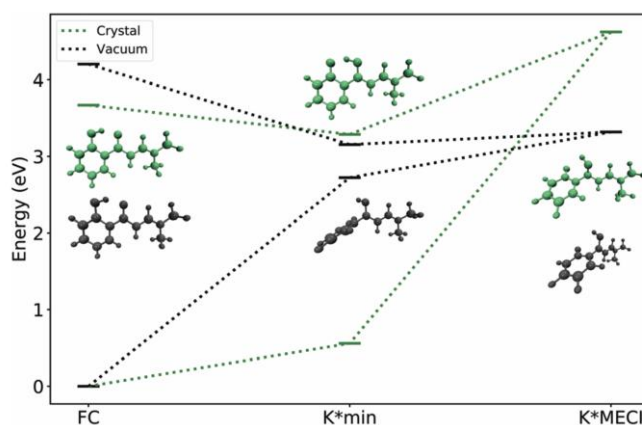


**Figure 6.** Energy diagram of one ESIPT dye comparing the relative energies of the keto minimum and related CI (noted K\*MECI). Reproduced from Ref. 50c. Copyright 2020 the Royal Society of Chemistry. See the original work for technical details.

## Lasing

### *Light amplification in multilevel systems*

The basic two-level system consists of two energy states: ground and excited, in which, the majority of atoms of a given material are in the lowest energy state **1**, while the rest lies in the excited state **2**, according to the thermodynamic equilibrium (Figure 7a). When we try to perform an inversion of population in such a system, that is mandatory for the LASER effect, we reach the saturation of the transition (50% of the molecules in the ground state and 50% of the molecule at the excited state) instead of the inversion, and it is not possible to obtain a lasing action.<sup>52</sup>

The involvement of a third energy level greatly facilitates the inversion of occupations, *i.e.*, the state in which most atoms are in an excited instead of a ground state. In this case, it is more likely that the emitted photon encounters an excited atom, leading to cascading stimulated emission instead of absorption, which can be used for laser action. This condition is met in a three-level system where absorption results in excitation to a higher energy state **2**, followed by rapid relaxation to a metastable state **3** (Figure 7b). If enough atoms have left the ground state **1** due to excitation, the interconversion between states **2** and **3** being fast, and state **3** has a large enough lifetime, then laser action occurs between states **3** and **1**. However, continuous operation is very difficult to achieve in three-level systems, whereas it becomes highly facilitated in a four-level system, where the laser action takes place between state **3** and an additional metastable state **4**, with  $E_1 < E_4 < E_3$  (Figure 7c).

ESIPT dyes represent attractive compounds to achieve four-level systems. ESIPT materials, since the pioneer works by Kierstead in 1970 and Kasha in 1984,<sup>53</sup> have attracted much attention as the active medium necessary for the lasing action. This long interval between the two papers (14 years!) becomes understandable when looking at the first work. The laser action observed by Kierstead did not appear groundbreaking, and in

addition, the species involved in the light amplification were not identified at that time. It was only when Kasha combined the laser action with the ESIPT photocycle of the 3-hydroxyflavone that researchers' attention was drawn in that direction. A significant increase of interest in the following years arose from the comparison between the ESIPT four-level photocycle and the four-level of laser systems (Figure 7c). In the ESIPT, after pumping, the excited molecule undergoes a very rapid tautomerization to the  $T^*$  form, which relaxes through radiative pathways, returns to the ground state (N), allowing the N form to be re-excited. The fast kinetics of  $N^* \rightarrow T^*$  and  $T \rightarrow N$  tautomerization corresponds to the non-radiative deactivations from higher excited states in the four-level laser system ( $2 \rightarrow 3$ ,  $4 \rightarrow 1$ ), while the energy levels of the N and T forms correspond to the relevant states taking part in the laser action. As the tautomer is unstable when relaxed (state T), its population is obviously zero, which allows for laser action between the excited and the ground levels. For this reason, ESIPT compounds can be regarded as *natural-born* materials for lasing.<sup>54</sup>

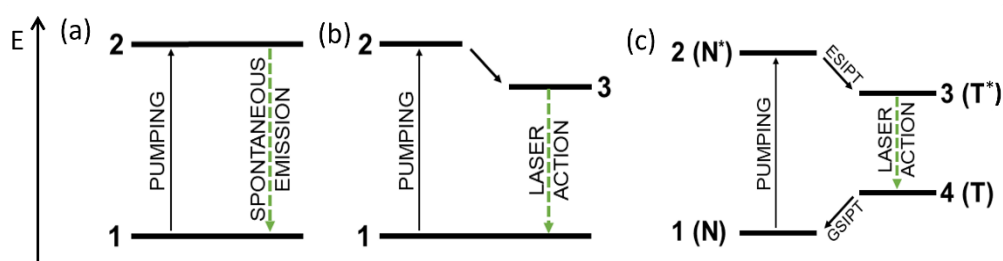


**Figure 7.** (a) Two-, (b) three- and (c) four-level laser system and ESIPT photocycle: N – normal, T – tautomer. Pumping corresponds to the excitation process. GS IPT = ground-state intramolecular proton transfer

### *A short history of ESIPT-based lasers*

From a historical point of view, the vast majority of the ESIPT-related light amplification investigations were focused on developing new materials and their Amplified Spontaneous Emission (ASE) properties in solution or solid-state, as reviewed by Liao in 2020.<sup>55</sup> As in the aforementioned works by Kasha and Kierstead, the first experiments were conducted on concentrated solutions contained in specifically designed cells, which worked as the cavity. Out of many ESIPT-type chromophores, some molecular scaffolds showing great performance in light amplification can be highlighted: 3-hydroxyflavones (3-HF),<sup>53,56–58</sup> salicylates,<sup>52,59,60</sup> 2-(2-hydroxyphenyl)imidazole (HPI),<sup>61–63</sup> 2-hydroxychalcone<sup>64–66</sup> or notable HBX derivatives.<sup>67–69</sup> The latter, when substituted with a fluorine, was used as a dopant in polymeric thin films, leading to the first observation of solid-state lasing action from an ESIPT dye.<sup>70</sup> This pioneer work was followed by numerous contributions on the application of ESIPT compounds either as dopants or as crystals.<sup>71,72</sup>

### *Solid-state emission, amplified spontaneous emission, and lasing*

While the four-level system of ESIPT luminescence is clearly very advantageous for laser action, ESIPT dyes are also investigated as environment-responsive sensors due to their inherent and sensitive intramolecular hydrogen bond.<sup>7a-b, 9b</sup> Their optical profile can be fine-tuned with various external stimuli, such as temperature, electrical current, humidity and environmental polarity variations.<sup>73,74</sup> Hence, besides the well-known spectral properties-chemical structure modifications, other paths for emission manipulation are open, .e.g., through co-crystal formation, as shown by Lin *et al.*,<sup>75</sup> leading to  $E^*/K^*$  emission tuning in solid-state. They did not investigate the light amplification phenomena, but nonetheless, organic structures obtained in such a way can still be applied in lasing. A prime example can be made on co-crystal lasers,<sup>76</sup> which were designed as halogen acceptor-donor pairs. Chu *et al.* reported tuning of lasing action through a change of the halogen donor, which resulted in precise tailoring of the energy levels, and subsequent cavity structures. An ESIPT type molecule served as acceptor, making it possible to obtain lasing of Fabry-Perot or Whispering Gallery Mode (WGM) types (Figure 8).

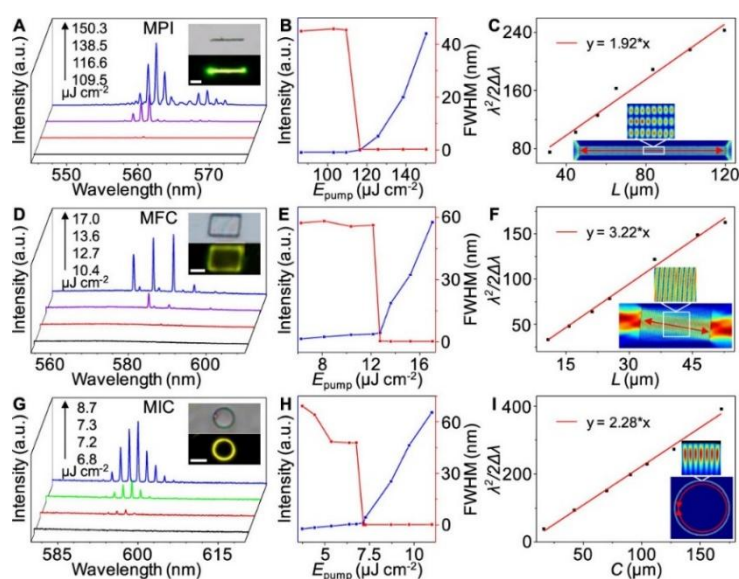


**Figure 8.** Optically pumped lasing measurements. (A,D,G) PL spectra of a single MPI wire (A), MFC plate (D), and MIC ring (G) pumped at different energies. Insets: Bright-field and PL images of a single wire, plate, and ring. Scale bars are 20, 5, and 20  $\mu\text{m}$ . (B,E,H) Power-dependent profiles of the PL intensities (blue) and fwhm (red) of the MPI (B), MFC (E), and MIC (H). (C,F,I) Plot and fitted curve of  $\lambda 2/2\Delta\lambda$  ( $\lambda = 559 \text{ nm}$ ) vs the length of the MPI wires (C),  $\lambda 2/2\Delta\lambda$  ( $\lambda = 581 \text{ nm}$ ) vs the length of the MFC plates (F) and  $\lambda 2/\pi\Delta\lambda$  ( $\lambda = 594 \text{ nm}$ ) vs. the circumference of the rings (I). Insets: Simulated electric field intensity distributions in the wire, plate, and ring cavity.<sup>76</sup> Reprinted with permission from Ref. 76. Copyright 2018 American Chemical Society.

Wire-like structures are often investigated in organic-based lasers, as such one-dimensional construction can act as a Fabry-Perot resonator.<sup>77,78</sup> One of the most notable works evidenced wavelength-switchable laser based on a HBT dye microwire.<sup>69</sup> Such feature was accomplished through photoisomerization of the HBT

molecule: depending on the conformation either 514 or 537 nm single-mode laser lines were obtained, for planar and twister *cis*-keto forms respectively (Figure 9). A molecule derived from HBT was also investigated as a dopant in the 5CB matrix, and as a precursor for a novel liquid crystal.<sup>77</sup> The liquid crystals' ability was exploited to orient the molecules with the external electric field, which was combined with the inherent light amplification affinity of the ESIPT chromophore. Hence, it was possible to modulate the ASE behavior electrically.

The crystallization has a major impact on the lasing properties of organic compounds. 1,5-dihydroxyanthraquinone (1,5-DHAQ) tends to form aggregates exhibiting four overlapping bands in the emission spectrum, corresponding to the fluorescence of N\* and T\* forms.<sup>78,79</sup> Single crystals obtained from this compound exhibit a square-like morphology of high quality, making it possible to apply them as WGM cavities. The same compound was also investigated as 1D arrays with controlled geometry,<sup>78</sup> leading to deep-red lasers of a high quality factor ( $Q > 2200$ ) and low lasing thresholds (Figure 10), which can, in addition, serve as vapor sensors or waveguides.

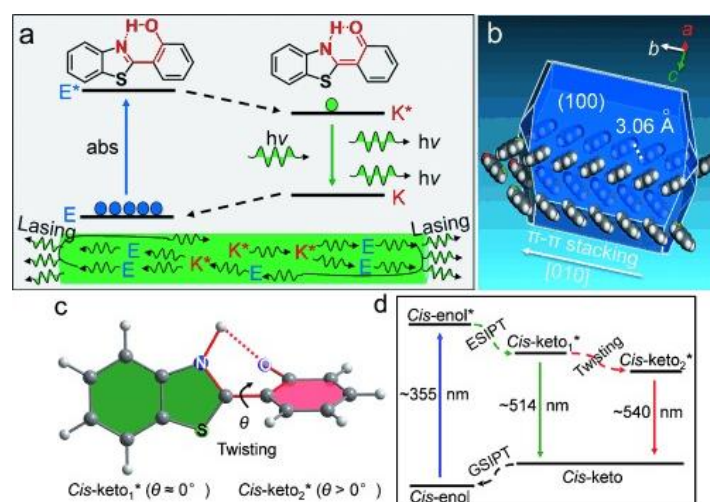


**Figure 9.** (a) Illustration of ESIPT four-level gain process based on the enol–keto phototautomerization of a model compound HBT. (b) Theoretically predicted growth morphology of a HBT crystal based on the attachment energies calculated with Material Studio package. The predicted growth thermodynamic stable morphology is 1D wire-like structure growing along the b axis. (c) Planar (*cis*-keto<sub>1</sub>\*) and twisted (*cis*-keto<sub>2</sub>\*) keto excited states.  $\theta$  is the twist angle between the benzothiazole ring and the hydroxyphenyl ring. (d) ESIPT photocycle in the HBT nanowires with two *cis*-keto\* states.<sup>69</sup> Adapted with permission from Ref. 69. Copyright 2015. John Wiley and Sons.

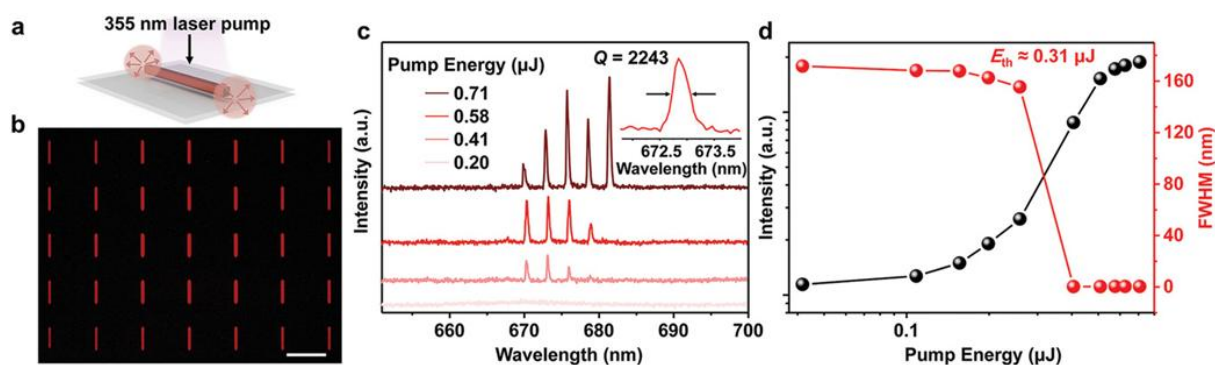


**Figure 10.** Lasing performance of 1D 1,5-DHAQ single-crystalline arrays. a) Schematic diagram of the Fabry–Pérot cavity in an organic microwire excited by a 355 nm pulsed laser beam. b) Fluorescence microscope image of assembled organic 1D arrays with length of 30  $\mu\text{m}$ . c) PL spectra using an individual organic microwire with  $L = 30 \mu\text{m}$ , which excited at different pump energies from 0.20 to 0.71  $\mu\text{J}$ . Right inset: Zoom-in PL spectrum of the organic microwire excited at 0.71  $\mu\text{J}$ . d) Pumping energy dependent plots of integrated intensities (black balls) and FWHM (red balls). Scale bar: b) 50  $\mu\text{m}$ .<sup>78</sup> Reprinted with permission from Ref. 78. Copyright 2022. John Wiley and Sons.

No sensing ability with these arrays during lasing action was mentioned, even though such development could likely be the next step, as the involvement of light amplification in detection has several advantages compared to the conventional one based on spectrometric methods, *e.g.* the obtained signal has a better signal-to-noise ratio – thus higher resolution, and the device sensitivity is also much higher. In 2016, another group investigated a different HPI-based ES IPT molecule,<sup>63</sup> which was also proven to work as a colorimetric vapor sensor. The interaction of alcohol vapors with the compound during the crystallization process led to five distinct crystal forms, varying in fluorescence intensity and position of the maximum wavelength. One of these structures was investigated as a potential active material for laser applications; the C1 was found to exhibit an ASE phenomenon, with an emission maximum located at *ca.* 500 nm (Figure 11).



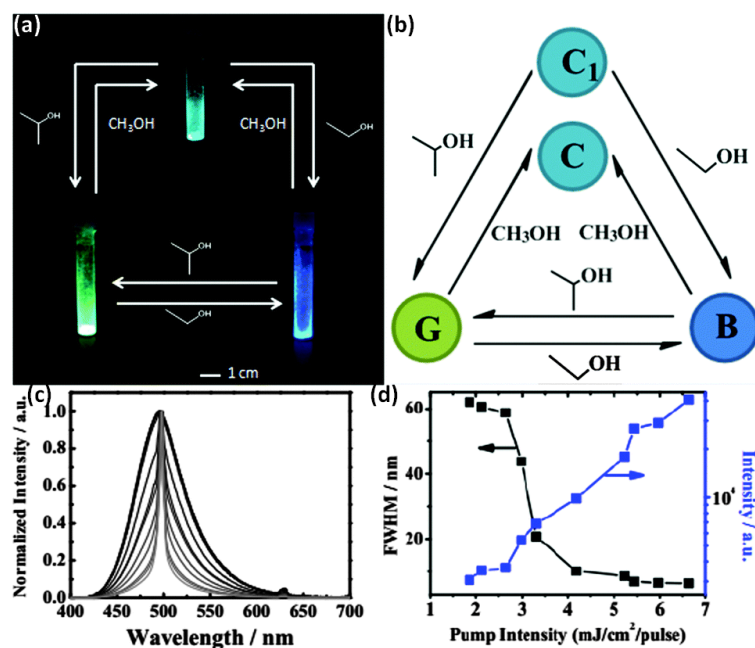


**Figure 11.** (a) Photograph of the luminescence tuning cycle by three alcohol vapors and (b) schematic illustration of the crystal changing process of H2hpi2cf during the fluorescence color tuning based on the PXRD patterns. (c) PL spectra as a function of the pump laser energy and (d) dependence of the peak intensity and FWHM of emission spectra of the C<sub>1</sub>-form crystal.<sup>63</sup> Adapted from Ref. 63. Copyright 2016 the Royal Society of Chemistry.

Emission tuning of the ESIPT process in solid-state can be also achieved by exploiting the polymorphic abilities of these materials, analogous to organic ICT compounds,<sup>80,81</sup> and this was already presented on 1-hydroxy-2-acetonaphthone derivative.<sup>82</sup> In 2016, Cheng *et al.* investigated hydroxyphenyl-based compounds,<sup>80</sup> which could crystallize into two polymorphs: 1 R and 1 O. The former exhibited emission in the NIR region, whereas for its counterpart, the spectrum was significantly blueshifted. The 1 O showed not only affinity towards protonation (when crystallized with hydrochloric acid), but also predisposition to temperature-induced polymorphism. Hence, three forms of the single compound were obtained and successfully used in ASE experiments.

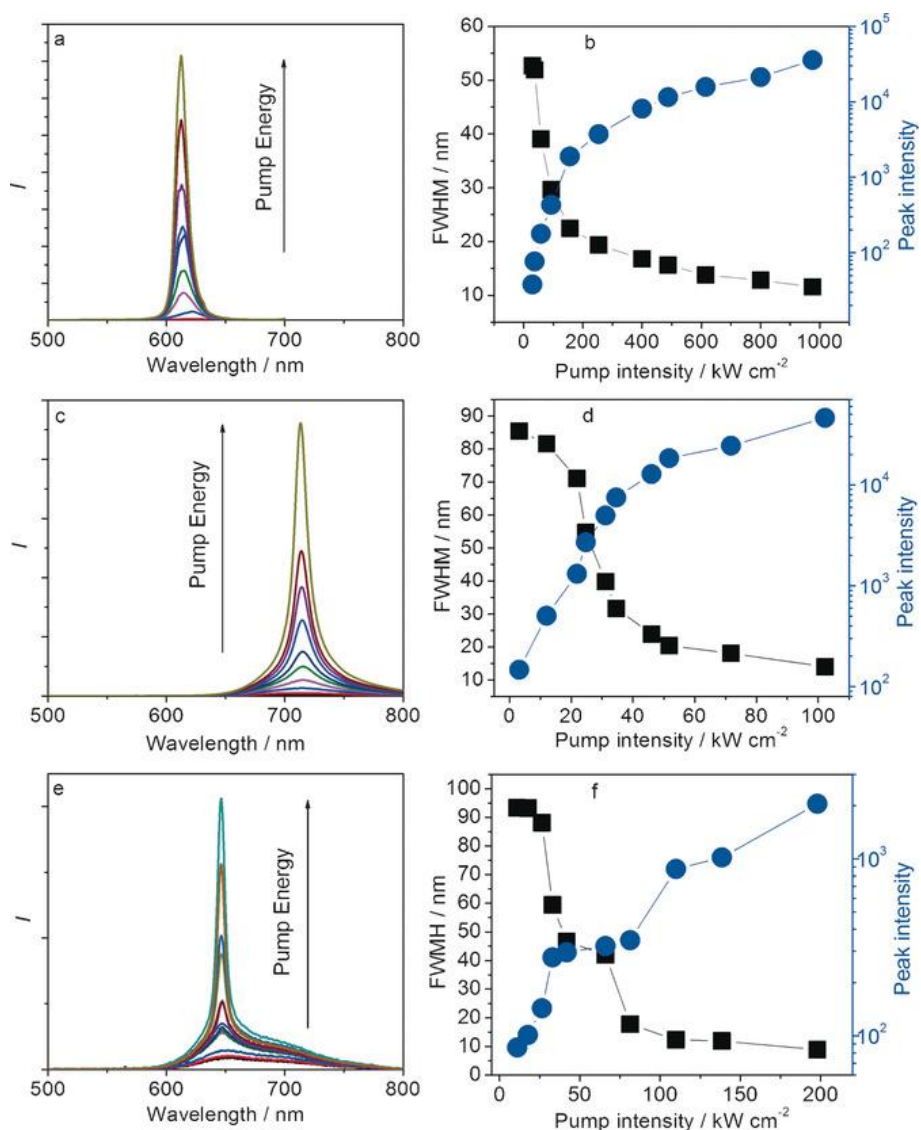


**Figure 12.** a), c), e) PL spectra as a function of the pump laser energy and dependence of the peak intensity and b), d) f) FWHM of emission spectra of 1 O (a, b), 1 R (c, d) and heated 1 O (e, f). The crystal sizes are about 0.5 mm×1 mm×0.8 μm (1 O), 3 mm×2 mm×0.03 mm (1 R), and 0.5 mm×1 mm×0.8 μm (heated 1 O).<sup>80</sup> Reprinted with permission from Ref. 80. Copyright 2016. John Wiley and Sons.

Efficient light confinement in the crystals made it possible to obtain stimulated emission at 612, 650, and 714 nm (for 1 O, 1 O – heated, and 1 R, respectively – Figure 12). Moreover, the emission of heated 1 O shifted towards shorter wavelengths upon grinding. All forms were capable of proton transfer in the excited state, ensuring a four-level system when applied in light amplification devices.

Information about solid-state ESIPT emitters for light amplification is presented in Table 1.

**Table 1.** Summary of lasing properties of exemplary ESIPT-based devices.

Material	Resonator	Shape	Pumping conditions	$\lambda_{cm}$ [nm]	Threshold	Q value	Ref.
<b>H<sub>2</sub>hpi<sub>2</sub>cf (C1)</b>	ASE	disk	355 nm, ns	500	600 kWcm <sup>-2</sup>	-	63
<b>HBT</b>	FP	wire	355 nm, fs	514	197 nJcm <sup>-2</sup>	1500	66
<b>MPI:F4DIB</b>	FP	plate	400 nm, fs	580	12.74 $\mu$ Jcm <sup>-2</sup>	1800	76
<b>MPI</b>	FP	wire	400 nm, fs	560	116.5 $\mu$ Jcm <sup>-2</sup>	2300	76
<b>MPI:IFB</b>	WGM	ring	400 nm, fs	600	7.1 $\mu$ Jcm <sup>-2</sup>	4500	76
<b>C<sub>5</sub>Ph-HBT/5CB</b>	ASE	LC blend	355 nm, ns	557	20 mJcm <sup>-2</sup>	-	77
<b>1,5-DHAQ</b>	FP	wire	355 nm, ns	673	0.31 $\mu$ J	2243	78
<b>1,5-DHAQ</b>	WGM	disk	355 nm, ns	672	0.39 $\mu$ J	2033	79
<b>1O</b>	ASE	crystal	355 nm, ns	612	37.1 kWcm <sup>-2</sup>	-	80
<b>Heated-1O</b>	ASE	crystal	355 nm, ns	653	26.4 kWcm <sup>-2</sup>	-	80
<b>1R</b>	ASE	crystal	355 nm, ns	714	20.8 kWcm <sup>-2</sup>	-	80

## Conclusions and future perspectives

In conclusion, it is relatively clear that papers published in the last few years show newly emerging research trends for ESIPT compounds, showing intense fluorescence emission in multiple environment on one hand but also acting as organic laser on the other hand. For the former, ab initio calculations appear as indispensable tools for the rationalization of the experimental results and the elaboration of future dyes. For the latter, the characteristic four-level photocycle of the ESIPT process is a positive addition, but current work is underway to engineer spectrally tunable emission in real-time, which could in turn affect the intensity ratio of N<sup>\*</sup>/T<sup>\*</sup> tautomers. The fact of being able to tune the stimulated emission in real-time will be very significant for the development of organic lasers, increasing their competitiveness compared to their widely used inorganic counterparts. Moreover, the innate sensory abilities of ESIPT dyes may be one possible way of implementing such devices, since to the best of our knowledge, the possibility of obtaining stimulated emission has not been successfully applied in sensing. Such application would be highly desired, as such devices would be characterized by high resolution sensitivity. On the other hand, panchromatic lasers are another possibility. As it was shown, desired stimulated emission spectra can be quite easily engineered, making it possible to fit the properties of the final device to the desired application. White emission and the corresponding Li-Fi (Light Fidelity) implementation can be highlighted in this regard. The Li-Fi systems which utilizes light to transmit data and position between devices, is based on the idea of white light emission with an examination of LEDs as a medium. This technology is now the subject of extensive research and testing.

Similarly, ESIPT dyes can be used in bioimaging, since many of these compounds, such as salicylic acid, are biocompatible and non-toxic. Appropriate modification of the chemical structure of the dyes makes it possible

to adjust the properties of these compounds so that they fit the target application, *e.g.* emission in the biological window.

## References

- (1) N. Amdursky, Y. Lin, N. Aho, G. Groenhof. Exploring fast proton transfer events associated with lateral proton diffusion on the surface of membranes. *Proc. Natl. Acad. Sci. U.S.A.* 2019, **116**, 2443-2451.
- (2) (a) J. Zhao, S. Ji, Y. Chen, H. Guo, P. Yang, Excited state intramolecular proton transfer (ESIPT): from principal photophysics to the development of new chromophores and applications in fluorescent molecular probes and luminescent materials. *Phys. Chem. Chem. Phys.*, 2012, **14**, 8803-8817. (b) C.-L. Chen, Y.-T. Chen, A. P. Demchenko, P.-T. Chou. Amino proton donors in excited-state intramolecular proton-transfer reactions. *Nat. Chem. Rev.*, 2018, **2**, 131-143.
- (3) N.N.M.Y. Chan, A. Idris, Z.H.Z. Abidin, H.A. Tajuddina, Z. Abdullah. White light employing luminescent engineered large (mega) Stokes shift molecules: a review. *RSC Adv.*, 2021, **11**, 13409-13444.
- (4) (a) T. Förster. Excimers. *Angew. Chem., Int. Ed.*, 1969, **8**, 5, 333-343. (b) M. Tasior, D. Kim, S. Singha, M. Krzeszewski, K.H. Ahn, D.T. Gryko.  $\pi$ -Expanded coumarins: synthesis, optical properties and applications. *J. Mater. Chem. C*, 2015, **3**, 1421-1446.
- (5) (a) J. Mei, N. L. Leung, R. T. Kwok, J. W. Lam, B.Z. Tang, Aggregation-Induced Emission: Together We Shine, United We Soar!. *Chem. Rev.* 2015, **115**, 11718-11940. (b) Z. Zhao, H. Zhang, J.W.Y. Lam, B.Z. Tang, Aggregation-Induced Emission: New Vistas at the Aggregate Level. *Angew. Chem., Int. Ed.*, **2020**, **59**, 9888-9907.
- (6) (a) J. Jiang, H. Sun, Y. Hu, G. Lu, J. Cui, J. Hao. AIE + ESIPT activity-based NIR Cu<sup>2+</sup> sensor with dye participated binding strategy. *Chem. Commun.*, 2021, **57**, 7685-7688. (b) R. Long, C. Tang, Z. Yang, Q. Fu, J. Xu, C. Tong, S. Shi, Y. Guo, D. Wang. A natural hyperoside based novel light-up fluorescent probe with AIE and ESIPT characteristics for on-site and long-term imaging of  $\beta$ -galactosidase in living cells. *J. Mater. Chem. C*, 2020, **8**, 11860-11865. (c) T. Stoerkler, P. Retailleau, D. Jacquemin, G. Ulrich, J. Massue. Heteroaryl-Substituted bis-Anils: Aggregation-Induced Emission (AIE) Derivatives with Tunable ESIPT Emission Color and pH Sensitivity. *Chem. Eur. J.*, 2023, **29**, e202203766.
- (7) (a) V.S. Padalkar, S. Seki, Excited-state intramolecular proton-transfer (ESIPT)-inspired solid state emitters. *Chem. Soc. Rev.*, 2016, **45**, 169-202. (b) L. Chen, P.-Y. Fu, H.-P. Wang, M. Pan. Excited-State Intramolecular Proton Transfer (ESIPT) for Optical Sensing in Solid State. *Adv. Opt. Mater.*, 2021, **9**, 23, 2001952. (c) M.K. Bera, P. Pal, S. Malik. Solid-state emissive organic chromophores: design, strategy and building blocks. *J. Mater. Chem. C*, 2020, **8**, 788-802.
- (8) J. Massue, D. Jacquemin, G. Ulrich. Molecular Engineering of Excited-state Intramolecular Proton Transfer (ESIPT) Dual and Triple Emitters. *Chem. Lett.*, 2018, **47**, 9, 1083-1089

- (9) (a) P. Gayathri, M. Pannipara, A.G. Al-Sehemi, S.P. Anthony. Recent advances in excited state intramolecular proton transfer mechanism-based solid state fluorescent materials and stimuli-responsive fluorescence switching. *CrystEngComm.*, 2021, **23**, 3771-3789. (b) A.C. Sedgwick, L. Wu, H.-H. Han, S.D. Bull, X.-P. He, T.D. James, J.L. Sessler, B.Z. Tang, H. Tian, J. Yoon. Excited-state intramolecular proton-transfer (ESIPT) based fluorescence sensors and imaging agents. *Chem. Soc. Rev.*, 2018, **47**, 8842-8880.
- (10) (a) E. Heyer, K. Benelhadj, S. Budzák, D. Jacquemin, J. Massue, G. Ulrich. On the Fine-Tuning of the Excited-State Intramolecular Proton Transfer (ESIPT) Process in 2-(2'-Hydroxybenzofuran)benzazole (HBBX) Dyes. *Chem. Eur. J.* 2017, **23**, 7324-7336. (b) S.K. Behera, S.Y. Park, J. Gierschner. Dual Emission: Classes, Mechanisms, and Conditions. *Angew. Chem., Int. Ed.*, 2021, **60**, 42, 22624-22638. (c) C. Azarias, S. Budzak, A. D. Laurent, G. Ulrich, D. Jacquemin. Tuning ESIPT fluorophores into dual emitters. *Chem. Sci.*, 2016, **120**, 3763-3774.
- (11) (a) T. Pariat, P.M. Vérité, D. Jacquemin, J. Massue, G. Ulrich. 2,2-Dipicolylamino substituted 2-(2'-hydroxybenzofuranyl) benzoxazole (HBBO) derivative: Towards ratiometric sensing of divalent zinc cations. *Dyes Pigm.*, 2021, **190**, 109338. (b) L. Wu, Y. Wang, M. Weber, L. Liu, A.C. Sedgwick, S.D. Bull, C. Huang, T.D. James. ESIPT-based ratiometric fluorescence probe for the intracellular imaging of peroxyinitrite. *Chem. Commun.*, 2018, **54**, 9953-9956. (c) G. Zeng, Z. Liang, X. Jiang, T. Quan, T. Chen. An ESIPT-Dependent AIE Fluorophore Based on HBT Derivative: Substituent Positional Impact on Aggregated Luminescence and its Application for Hydrogen Peroxide Detection. *Chem. Eur. J.*, 2022, **28**, 5, e202103241. (d) L. Wu, L. Liu, H.-H. Han, X. Tian, M.L. Odyniec, L. Feng, A.C. Sedgwick, X.-P. He, S.D. Bull, T.D. James. ESIPT-based fluorescence probe for the ratiometric detection of superoxide. *New J. Chem.*, 2019, **43**, 2875-2877.
- (12) (a) S. Kundu, B. Sk, P. Pallavi, A. Giri, A. Patra. Molecular Engineering Approaches Towards All-Organic White Light Emitting Materials. *Chem. Eur. J.*, 2020, **26**, 25, 5557-5582. (b) K. Benelhadj, W. Muzuzu, J. Massue, P. Retailleau, A. Charaf-Eddin, A.D. Laurent, D. Jacquemin, G. Ulrich, R. Ziessel, White Emitters by Tuning the Excited-State Intramolecular Proton-Transfer Fluorescence Emission in 2-(2'-Hydroxybenzofuran)benzoxazole Dyes. *Chem. Eur. J.*, 2014, **20**, 12843-12857.
- (13) (a) A.P. Demchenko, K.-C. Tang, P.-T. Chou. Excited-state proton coupled charge transfer modulated by molecular structure and media polarization. *Chem. Soc. Rev.*, 2013, **42**, 1379-1408. (b) M. Munch, E. Colombain, T. Stoerkler, P.M. Vérité, D. Jacquemin, G. Ulrich, J. Massue. Blue-Emitting 2-(2'-Hydroxyphenyl)benzazole Fluorophores by Modulation of Excited-State Intramolecular Proton Transfer: Spectroscopic Studies and Theoretical Calculations. *J. Phys. Chem. B*, 2022, **126**, 2108-2118. (c) M. Raoui, J. Massue, C. Azarias, D. Jacquemin, G. Ulrich. Highly fluorescent extended 2-(2'-hydroxyphenyl)benzazole dyes: synthesis, optical properties and first-principle calculations. *Chem. Commun.*, 2016, **52**, 59, 9216-9219.
- (14) (a) M. Munch, M. Curtil, P.M. Vérité, D. Jacquemin, J. Massue, G. Ulrich. Ethynyl-Tolyl Extended 2-(2'-Hydroxyphenyl)benzoxazole Dyes: Solution and Solid-state Excited-State Intramolecular Proton Transfer (ESIPT) Emitters. *Eur. J. Org. Chem.*, 2019, 1134-1144. (b) K.-I. Sakai, T. Ishikawa, T. Akutagawa. A blue-white-yellow color-tunable excited state intramolecular proton transfer (ESIPT) fluorophore: sensitivity to polar-nonpolar solvent ratios. *J. Mater. Chem. C*, 2013, **1**, 47, 7866-7871.

- (15) (a) K. Skonieczny, J. Yoo, J.M. Larsen, E.M. Espinoza, M. Barbasiewicz, V.I. Vullev, C.-H. Lee, D.T. Gryko. How To Reach Intense Luminescence for Compounds Capable of Excited-State Intramolecular Proton Transfer? *Chem. Eur. J.* 2016, **22**, 7485-7496. (b) T. Stoerkler, D. Frath, D. Jacquemin, J. Massue, G. Ulrich. Dual-State Emissive  $\pi$ -Extended Salicylaldehyde Fluorophores: Synthesis, Photophysical Properties and First-Principle Calculations. *Eur. J. Org. Chem.*, 2021, **26**, 3726-3736. (c) M. Zhang, R. Cheng, J. Lan, H. Zhang, L. Yan, X. Pu, Z. Huang, D. Wu, J. You. Oxidative C-H/C-H Cross-Coupling of [1,2,4]Triazolo[1,5-a]pyrimidines with Indoles and Pyrroles: Discovering Excited-State Intramolecular Proton Transfer (ESIPT) Fluorophores. *Org. Lett.*, 2019, **21**, 4058-4062.
- (16) (a) D. Yao, S. Zhao, J. Guo, Z. Zhang, H. Zhang, Y. Liu, Y. Wang, Hydroxyphenyl-benzothiazole based full color organic emitting materials generated by facile molecular modification. *J. Mater. Chem.*, 2011, **21**, 3568-3570. (b) K.-I. Sakai, T. Ishikawa, T. Akutagawa, A blue-white-yellow color-tunable excited state intramolecular proton transfer (ESIPT) fluorophore: sensitivity to polar-nonpolar solvent ratios *J. Mater. Chem. C*, 2013, **1**, 47, 7866-7871. (c) K. Benelhadj, J. Massue, G. Ulrich, 2,4 and 2,5-bis(benzooxazol-2'-yl)hydroquinone (DHBO) and their borate complexes: synthesis and optical properties. *New J. Chem.*, 2016, **40**, 7, 5877.
- (18) (a) T. Stoerkler, T. Pariat, A.D. Laurent, D. Jacquemin, G. Ulrich, J. Massue. Excited-State Intramolecular Proton Transfer Dyes with Dual-State Emission Properties: Concept, Examples and Applications. *Molecules*, 2022, **27**, 2443. (b) J.L. Belmonte-Vazquez, Y.A. Amador-Sanchez, L.A. Rodriguez-Cortes, B. Rodriguez-Molina. Dual-State Emission (DSE) in Organic Fluorophores: Design and Applications. *Chem. Mater.*, 2021, **33**, 7160-7184. (c) A. Huber, J. Dubbert, T.D. Scherz, J. Voskuhl. Design Concepts for Solution and Solid-State Emitters—A Modern View point on Classical and Non-Classical Approaches. *Chem. Eur. J.*, 2023, **29**, e2022024.
- (19) I.D.W. Samuel, G.A. Turnbull. Organic Semiconductor Lasers *Chem. Rev.* 2007, **107**, 1272-1295.
- (20) L. Zou, S. Guo, H. Lv, F. Chen, L. Wei, Y. Gong, Y. Liu, C. Wei. Molecular design for organic luminogens with efficient emission in solution and solid-state. *Dyes Pigm.* 2022, **198**, 109958
- (21) N. Venkatramaiah, G.D Kumar, Y. Chandrasekaran, R. Ganduri, S. Patil. Efficient Blue and Yellow Organic Light-Emitting Diodes Enabled by Aggregation-Induced Emission. *ACS Appl. Mat. & Interfaces*, 2018, **10**, 3838-3847.
- (22) Y. Xu, L. Ren, D. Dang, Y. Zhi, X. Wang, L. Meng. A Strategy of "Self-Isolated Enhanced Emission" to Achieve Highly Emissive Dual-State Emission for Organic Luminescent Materials. *Chem. Eur. J.*, 2018, **24**, 41, 10383-10389.
- (23) K. Ohno, F. Narita, H. Yokobori, N. Iiduka, T. Sugaya, A. Nagasawa, T. Fujihara. Substituent effect on emission of flavonolate-boron difluoride complexes: The role of  $\pi$ -system for dual-state (solution and solid) emission. *Dyes Pigm.*, 2021, **187**, 109081.
- (24) Z. Xiang, Z.-Y. Wang, T.-B. Ren, W. Xu, Y.-P. Liu, X.-X. Zhang, P. Wu, L. Yuan, X.-B. Zhang. A general strategy for development of a single benzene fluorophore with full-color-tunable, environmentally insensitive, and two-photon solid-state emission. *Chem. Commun.*, 2019, **55**, 76, 11462-11465.

- (25) X.-L. Peng, S. Ruiz-Barragan, Z.-S. Li, Q.-S. Li, L. Blancafort. Restricted access to a conical intersection to explain aggregation induced emission in dimethyl tetraphenylsilole. *J. Mater. Chem. C*, 2016, **4**, 14, 2802-2810.
- (26) (a) J. Massue, A. Felouat, M. Curtil, P.M. Vérité, D. Jacquemin, G. Ulrich. Solution and Solid-State Excited-State Intramolecular Proton Transfer (ESIPT) emitters incorporating Bis-triethyl- or triphenylsilylethynyl units. *Dyes Pigm.*, 2019, **160**, 915-922. (b) T. Pariat, M. Munch, M. Durko-Maciag, J. Mysliwiec, P. Retailleau, P.M. Vérité, D. Jacquemin, J. Massue, G. Ulrich. Impact of Heteroatom Substitution on Dual-State Emissive Rigidified 2-(2'-hydroxyphenyl)benzazole Dyes: Towards Ultra-Bright ESIPT Fluorophores. *Chem. Eur. J.*, 2021, **27**, 10, 3483-3495.
- (27) T. Pariat, T. Stoerkler, C. Diguët, A.D. Laurent, D. Jacquemin, G. Ulrich, J. Massue. Dual Solution-/Solid-State Emissive Excited-State Intramolecular Proton Transfer (ESIPT) Dyes: A Combined Experimental and Theoretical Approach. *J. Org. Chem.*, 2021, **86**, 17606-17619.
- (28) T. Stoerkler, A.D. Laurent, G. Ulrich, D. Jacquemin, J. Massue. Influence of ethynyl extension on the dual-state emission properties of pyridinium-substituted ESIPT fluorophores. *Dyes Pigm.*, 2022, **208**, 110872.
- (29) D. Göbel, P. Rusch, D. Duvinage, T. Stauch, N.C. Bigall, B.J. Nachtsheim. Substitution Effect on 2-(Oxazoliny)-phenols and 1,2,5- Chalcogenadiazole-Annulated Derivatives: Emission-Color-Tunable, Minimalistic Excited-State Intramolecular Proton Transfer (ESIPT)- Based Luminophores. *J. Org. Chem.*, 2021, **86**, 14333-14355.
- (30) D. Göbel, D. Duvinage, T. Stauch, B.J. Nachtsheim. Nitrile-substituted 2-(oxazoliny)-phenols: minimalistic excited-state intramolecular proton transfer (ESIPT)-based fluorophores, *J. Mater. Chem. C*, 2020, **8**, 9213-9225.
- (31) K. Benelhadj, J. Massue, P. Retailleau, G. Ulrich, R. Ziessel. 2-(2'-Hydroxyphenyl)benzimidazole and 9,10-Phenanthroimidazole Chelates and Borate Complexes: Solution- and Solid-State Emitters. *Org. Lett.*, 2013, **15**, 2918-2921.
- (32) K. Takagi, Y. Yamada, R. Fukuda, M. Ehara, D. Takeuchi. ESIPT emission behavior of methoxy-substituted 2-hydroxyphenylbenzimidazole isomers. *New J. Chem.*, 2018, **42**, 8, 5923-5928.
- (33) K. Takagi, K. Ito, Y. Yamada, T. Nakashima, R. Fukuda, M. Ehara, H. Masu. Synthesis and Optical Properties of Excited-State Intramolecular Proton Transfer Active  $\pi$ -Conjugated Benzimidazole Compounds: Influence of Structural Rigidification by Ring Fusion. *J. Org. Chem.* 2017, **82**, 12173-12180.
- (34) J. Tian, D. Shi, Y. Zhang, X. Li, X. Li, H. Teng, T.D. James, J. Li, Y. Guo, Y. Stress response decay with aging visualized using a dual-channel logic-based fluorescent probe. *Chem. Sci.*, 2021, **12**, 40, 13483-13491
- (35) I. Kaur, Shivani; P. Kaur, K. Singh 2-(2'-Hydroxyphenyl)benzothiazole derivatives: Emission and color tuning. *Dyes Pigm.*, 2020, **176**, 108198.
- (36) M. Huang, J. Zhou, K. Xu, X. Zhu, Y. Wan. Enhancement of the excited-state intramolecular proton transfer process to produce all-powerful DSE molecules for bridging the gap between ACQ and AIE. *Dyes Pigm.*, 2019, **160**, 839-847.

- (37) V. Trannoy, A. Léaustic, S. Gadan, R. Guillot, C. Allain, G. Clavier, S. Mazerat, B. Geffroy, P.A. Yu. A highly efficient solution and solid state ESIPT fluorophore and its OLED application. *New J. Chem.*, 2021, **45**, 3014-3021.
- (38) C.C. Anghel, C. Badescu, A.G. Mirea, A. Paun, N.D. Nadade, A.M. Madalan, M. Matache, C.C. Popescu. Two are better than one - Synthesis of novel blue and green emissive hydroxy-oxadiazoles. *Dyes Pigm.*, 2022, **197**, 109927.
- (39) G. Xia, Q. Shao, K. Liang, Y. Wang, L. Jiang, H. Wang. A phenyl-removal strategy for accessing an efficient dual-state emitter in the red/NIR region guided by TDDFT calculations. *J. Mater. Chem. C*, 2020, **8**, 13621-13626.
- (40) J. Jankowska, A. L. Sobolewski, Modern Theoretical Approaches to Modeling the Excited-State Intramolecular Proton Transfer: An Overview. *Molecules*, 2021, **26**, 5140.
- (41) J. Tomasi, B. Mennucci, R. Cammi, R. Quantum Mechanical Continuum Solvation Models. *Chem. Rev.* 2005, **105**, 2999-3094.
- (42) (a) M. Caricato, Absorption and Emission Spectra of Solvated Molecules with the EOM-CCSD-PCM Method. *J. Chem. Theory Comput.* 2012, **8**, 4494-4502. (b) B. Lunkenheimer, A. Köhn, Solvent Effects on Electronically Excited States Using the Conductor-Like Screening Model and the Second-Order Correlated Method ADC(2). *J. Chem. Theory Comput.* 2013, **9**, 977-994. (c) J. M. Mewes, J. M. Herbert, A. Dreuw, On the Accuracy of the General, State-Specific Polarizable-Continuum Model for the Description of Correlated Ground- and Excited States In Solution. *Phys. Chem. Chem. Phys.* 2017, **19**, 1644-1654. (d) I. Duchemin, D. Jacquemin, X. Blase, Combining the GW Formalism with the Polarizable Continuum Model: A State-Specific Non-Equilibrium Approach. *J. Chem. Phys.* 2016, **144**, 164106. (e) I. Duchemin, C. A. Guido, D. Jacquemin, X. Blase, The Bethe-Salpeter formalism with polarizable continuum embedding: reconciling linear-response and state-specific features. *Chem. Sci.* 2018, **9**, 4430-4443.
- (43) C. A. Guido, S. Caprasecca, On the Description of the Environment Polarization Response to Electronic Transitions. *Int. J. Quantum Chem.* 2019, **119**, e25711.
- (44) R. Cammi, B. Mennucci, Linear response theory for the polarizable continuum model. *J. Chem. Phys.* 1999, **110**, 9877-9886.
- (45) M. Caricato, B. Mennucci, J. Tomasi, F. Ingrosso, R. Cammi, S. Corni, G. Scalmani, Formation and Relaxation of Excited States in Solution: A new Time Dependent Polarizable Continuum Model Based on Time Dependent Density Functional Theory. *J. Chem. Phys.* 2006, **124**, 124520.
- (46) (a) P. M. Vérité, C. A. Guido, D. Jacquemin, First-principles investigation of the double ESIPT process in a thiophene-based dye. *Phys. Chem. Chem. Phys.* 2019, **21**, 2307-2317. (b) C. A. Guido, A. Chrayteh, G. Scalmani, B. Mennucci, D. Jacquemin, Simple Protocol for Capturing Both Linear-Response and State-Specific Effects in Excited-State Calculations with Continuum Solvation Models. *J. Chem. Theo. Comput.* 2021, **17**, 5155-5164.



- (47) M. Nottoli, M. Bondanza, F. Lipparini, B. Mennucci, An enhanced sampling QM/AMOEBA approach: The case of the excited state intramolecular proton transfer in solvated 3-hydroxyflavone. *J. Chem. Phys.* 2021, **154**, 184107.
- (48) (a) J. Paterson, M. A. Robb, L. Blancafort, A. D. DeBellis. Theoretical Study of Benzotriazole UV Photostability: Ultrafast Deactivation through Coupled Proton and Electron Transfer Triggered by a Charge-Transfer State. *J. Am. Chem. Soc.* 2004, **126**, 2912-2922. (b) J. Paterson, M. A. Robb, L. Blancafort, A. D. DeBellis, Mechanism of an Exceptional Class of Photostabilizers: A Seam of Conical Intersection Parallel to Excited State Intramolecular Proton Transfer (ESIPT) in o-Hydroxyphenyl-(1,3,5)-triazine. *J. Phys. Chem. A* 2005, **109**, 7527-7537. (c) H. H. G. Tsai, H. L. S. Sun, C. Tan, C.-J. TD-DFT Study of the Excited-State Potential Energy Surfaces of 2-(2'-Hydroxyphenyl) benzimidazole and its Amino Derivatives. *J. Phys. Chem. A* 2010, **114**, 4065-4079.
- (49) (a) D. Presti, F. Labat, A. Pedone, M. J. Frisch, H. P. Hratchian, I. Ciofini, M. C. Menziani, C. Adamo, Modeling emission features of salicylidene aniline molecular crystals: A QM/QM' approach. *J. Comput. Chem.* 2016, **37**, 861-870. (b) D. Presti, A. Pedone, I. Ciofini, F. Labat, M. C. Menziani, C. Adamo, C. Optical properties of the dibenzothiazolylphenol molecular crystals through ONIOM calculations: the effect of the electrostatic embedding scheme. *Theor. Chim. Acta* 2016, **135**, 86. (c) D. Presti, L. Wilbraham, C. Targa, F. Labat, A. Pedone, M. C. Menziani, I. Ciofini, C. Adamo, C. Understanding Aggregation-Induced Emission in Molecular Crystals: Insights from Theory. *J. Phys. Chem. C* 2017, **121**, 5847-5752.
- (50) (a) M. Rivera, M. Dommett, R. Crespo-Otero ONIOM(QM:QM') electrostatic embedding schemes for photochemistry in molecular crystals. *J. Chem. Theor. Comput.* 2019, **15**, 2504-2516. (b) M. Rivera, M. Dommett, A. Sidat, W. Rahim, R. Crespo-Otero, Fromage: A library for the study of molecular crystal excited states at the aggregate scale. *J. Comput. Chem.* 2020, **41**, 1045-1058. (c) M. Dommett, M. Rivera, M. T. H. Smith, R. Crespo-Otero, Molecular and crystalline requirements for solid state fluorescence exploiting excited state intramolecular proton transfer. *J. Mater. Chem. C* 2020, **8**, 2558-2568.
- (51) (a) M. Dommett, M. Rivera, R. Crespo-Otero, How Inter- and Intramolecular Processes Dictate Aggregation-Induced Emission in Crystals Undergoing Excited-State Proton Transfer. *J. Phys. Chem. Lett.* 2017, **8**, 6148-6153. (b) Q. Zhang, Y. Li, Z. Cao, C. Zhu, Aggregation-induced emission spectra of triphenylamine salicylaldehyde derivatives via excited-state intramolecular proton transfer revealed by molecular spectral and dynamics simulations. *RSC Adv.* 2021, **11**, 37171-37180. (c) H. Wang, Q. Gong, G. Wang, J. Dang, F. Liu, F. Deciphering the Mechanism of Aggregation-Induced Emission of a Quinazolinone Derivative Displaying Excited-State Intramolecular Proton-Transfer Properties: A QM, QM/MM, and MD Study. *J. Chem. Theo. Comput.* 2019, **15**, 5440-5447. (d) J. Zhao, H. Dong, H. Yang, Y. Zheng, Aggregation Promotes Excited-State Intramolecular Proton Transfer for Benzothiazole-Substituted Tetraphenylethylene Compound. *ACS Appl. Bio Mater.* 2019, **2**, 5182-5189.
- (52) O. Svelto, Principles of lasers, 5<sup>th</sup> Ed., New York: Springer, 2010 .

- (53) (a) J.A. Myer, I. Itzkan, E. Kierstead. Dye Lasers in the Ultraviolet. *Nature*, 1970, **225**, 5232, 544-545.  
(b) P. Chou, D. McMorrow, T.J Aartsma, M. Kasha The Proton-Transfer Laser. Gain Spectrum and Amplification of Spontaneous Emission of 3-Hydroxyflavone. *J. Phys. Chem.* 1984, **88**, 20, 4596–4599
- (54) J. Massue, T. Pariat, P.M. Vérité, D. Jacquemin, M. Durko, T. Chtouki, L. Sznitko, J. Mysliwiec, G. Ulrich. Natural Born Laser Dyes: Excited-State Intramolecular Proton Transfer (ESIPT) Emitters and Their Use in Random Lasing Studies. *Nanomaterials*, 2019, **9**, 8, 1093.
- (55) C.-C. Yan, X.-D. Wang, L.-S. Liao. Organic Lasers Harnessing Excited State Intramolecular Proton Transfer Process. *ACS Photonics*, 2020, **7**, 6, 1355-1366.
- (56) D. Gormin, A. Sytnik, M Kasha. Spectroscopy of Amplified Spontaneous Emission Laser Spikes in Polyhydroxyflavones. *J. Phys. Chem. A*, 1997, **101**, 4, 672-677.
- (57) D.A. Arthenopoulos, D. P. McMorrow, M. Kasha. Comparative Study of Stimulated Proton-Transfer Luminescence of Three Chromones. *J. Phys. Chem.* 1991, **95**, 7, 2668-2674.
- (58) P.-T. Chou, M.L. Martinez, J.H. Clements. The Observation of Solvent-Dependent Proton-Transfer / Charge-Transfer Lasers from 4'-Diethylamino-3-Hydroxyflavone. *Chem. Phys. Lett.* 1993, **204**, 5-6, 395–399.
- (59) A.U. Acuña, F. Amat, J. Catalán, A. Costela, J.M. Figuera, J. M. Muñoz. Pulsed Liquid Lasers from Proton Transfer in the Excited State. *Chem. Phys. Lett.* 1986, **132**, 6, 567-569.
- (60) A.U. Acuña, A. Costela, J.M. Muñoz, A Proton-Transfer Laser. *J. Phys. Chem.* 1986, **90**, 13, 2807-2808.
- (61) S. Park, O-H. Kwon, S. Kim, S. Park, M.-G. Choi, M. Cha, S.Y. Park, D.-J. Jang. Imidazole-Based Excited-State Intramolecular Proton-Transfer Materials: Synthesis and Amplified Spontaneous Emission from a Large Single Crystal. *J. Am. Chem. Soc.* 2005, **127**, 28, 10070-10074.
- (62) H.H. Lim, S. Boomadevi, O.-Y. Jeon, K. Kyhm, M. Cha, S. Park, S.Y. Park. Polarization-Dependent Optical Gain in Crystal and Glass Composed of Excited-State Intramolecular Proton Transfer Organic Molecules. *Mater. Lett.* 2007, **61**, 19–20, 4213-4215.
- (63) L. Chen, S.-Y. Yin, M. Pan, K. Wu, H.-P. Wang, Y.-N. Fan, C.-Y. Su. A Naked Eye Colorimetric Sensor for Alcohol Vapor Discrimination and Amplified Spontaneous Emission (ASE) from a Highly Fluorescent Excited-State Intramolecular Proton Transfer (ESIPT) Molecule. *J. Mater. Chem. C* 2016, **4**, 29, 6962-6966.
- (64) X. Wang, Q. Liao, X. Lu, H. Li, Z. Xu, H. Fu, H. Shape-Engineering of Self-Assembled Organic Single Microcrystal as Optical Microresonator for Laser Applications. *Sci. Rep.* 2014, **4**, 1, 1-8.
- (65) J. Li, Y. Wu, Z. Xu, Q. Liao, H. Zhang, Y. Zhang, L. Xiao, J. Yao, H. Fu. Tuning the Organic Microcrystal Laser Wavelength of ESIPT-Active Compounds via Controlling the Excited Enol\* and Keto\* Emissions. *J. Mater. Chem. C* 2017, **5**, 46, 12235-12240.
- (66) X. Cheng, K. Wang, S. Huang, H. Zhang, H. Zhang, Y. Wang. Organic Crystals with Near-Infrared Amplified Spontaneous Emissions Based on 2'-Hydroxychalcone Derivatives: Subtle Structure Modification but Great Property Change. *Angew. Chem. Int. Ed.* 2015, **54**, 29, 8369-8373.
- (67) (a) J. Massue, A. Felouat, P.M. Vérité, D. Jacquemin, K. Cyprych, M. Durko, L. Sznitko, J. Mysliwiec, G. Ulrich. An Extended Excited-State Intramolecular Proton Transfer (ESIPT) Emitter for Random Lasing

Applications. *Phys. Chem. Chem. Phys.* 2018, **20**, 30, 19958-19963. (b) M. Durko-Maciag, D. Jacquemin, G. Ulrich, J. Massue, J. Mysliwiec. Color-Tunable Multifunctional Excited-State Intramolecular Proton Transfer Emitter: Stimulated Emission of a Single Dye. *Chem. Eur. J.*, 2022, **28**, 44, e202201327.

(68) C.E. Fellows, U. Tauber, C.C. Rodegheri, C.E.M. Carvalho, F.D. Acevedo, S.G. Bertolotti, C. Barbero. ASE and Photodegradation of Two Benzimidazole Derivatives Proton Transfer Dyes in Polymeric Matrices. *Opt. Mater.* 2004, **27**, 3, 499-502.

(69) W. Zhang, Y. Yan, J. Gu, J. Yao, Y.S. Zhao. Low-Threshold Wavelength-Switchable Organic Nanowire Lasers Based on Excited-State Intramolecular Proton Transfer. *Angew. Chem. Int. Ed.* 2015, **54**, 24, 7125-7129.

(70) A.U. Acuña, F. Amat-Guerri, A. Costela, A. Douhal, J.M. Figuera, F. Florido, R. Sastre. Proton-Transfer Lasing from Solid Organic Matrices. *Chem. Phys. Lett.* 1991, **187**, 1, 98-102.

(71) S. Park, J.E. Kwon, S.-Y. Park, O.-H. Kwon, J.K. Kim, S.-J. Yoon, J.W. Chung, D.R. Whang, S.K. Park, D.K. Lee, D.-J. Jang, J. Gierschner, S.Y. Park. Crystallization-Induced Emission Enhancement and Amplified Spontaneous Emission from a CF<sub>3</sub>-Containing Excited-State Intramolecular-Proton-Transfer Molecule. *Adv. Opt. Mater.* 2017, **5**, 18, 1700353.

(72) J. Wu, M. Zhuo, R. Lai, S. Zou, C. Yan, Y. Yuan, S. Yang, G. Wei, X. Wang, L. Liao. Cascaded Excited-State Intramolecular Proton Transfer Towards Near-Infrared Organic Lasers Beyond 850 nm. *Angew. Chem. Int. Ed.* 2021, **60**, 16, 9114-9119.

(73) J.E. Kwon, S.Y. Park. Advanced Organic Optoelectronic Materials: Harnessing Excited-State Intramolecular Proton Transfer (ESIPT) Process. *Adv. Mater.* 2011, **23**, 32, 3615-3642.

(74) P. Zhou, K. Han. ESIPT-Based AIE Luminogens: Design Strategies, Applications, and Mechanisms. *Aggregate* 2022, **3**, 5, e160.

(75) H. Lin, X. Chang, D. Yan, W.-H. Fang, G. Cui, G. Tuning Excited-State-Intramolecular-Proton-Transfer (ESIPT) Process and Emission by Cocrystal Formation: A Combined Experimental and Theoretical Study. *Chem. Sci.* 2017, **8**, 3, 2086-2090.

(76) M. Chu, B. Qiu, W. Zhang, Z. Zhou, X. Yang, Y. Yan, J. Yao, Y. Li, Y.S. Zhao. Tailoring the Energy Levels and Cavity Structures toward Organic Cocrystal Microlasers. *ACS Appl. Mater. Interfaces* 2018, **10**, 49, 42740-42746.

(77) Y. Tsutsui, W. Zhang, S. Ghosh, T. Sakurai, H. Yoshida, M. Ozaki, T. Akutagawa, S. Seki. Electrically Switchable Amplified Spontaneous Emission from Liquid Crystalline Phase of an AIEE-Active ESIPT Molecule. *Adv. Opt. Mater.* 2020, **8**, 14, 1902158.

(78) Y. Geng, Y. Zhao, Y. Zhao, F. Feng, J. Zhang, X. Fan, H. Gao, X.-D. Wang, L. Jiang, Y. Wu. Multifunctional Organic Single-Crystalline Microwire Arrays toward Optical Applications. *Adv. Funct. Mater.* 2022, **32**, 19, 2113025.

(79) G.-Q. Wei, Y. Yu, M.-P. Zhuo, X.-D. Wang, L.S. Liao. Organic Single-Crystalline Whispering-Gallery Mode Microlasers with Efficient Optical Gain Activated via Excited State Intramolecular Proton Transfer Luminogens. *J. Mater. Chem. C* 2020, **8**, 34, 11916-11921.

- (80) X. Cheng, Y. Zhang, S. Han, F. Li, H. Zhang, Y. Wang. Multicolor Amplified Spontaneous Emissions Based on Organic Polymorphs That Undergo Excited-State Intramolecular Proton Transfer. *Chem. - Eur. J.* 2016, **22**, 14, 4899-4903.
- (81) H. Dong, C. Zhang, J. Yao, Y.S. Zhao. Wavelength-Controlled Organic Microlasers Based on Polymorphism-Dependent Intramolecular Charge-Transfer Process. *Chem. – Asian J.* 2016, **11**, 19, 2656–2661.
- (82) X. Wang, Z.-Z. Li, S.-F. Li, H. Li, J. Chen, Y. Wu, H. Fu. Near-Infrared Organic Single-Crystal Lasers with Polymorphism-Dependent Excited State Intramolecular Proton Transfer. *Adv. Opt. Mater.* 2017, **5**, 12, 1700027.